NUMERICAL COMPUTATION OF THE ACOUSTIC RESPONSE OF AN ACTIVE AIRFOIL WITH IMPEDANCE BOUNDARY CONDITIONS TO A TURBULENT WAKE

Mouhamed Mounibe Ezzine, Jonathan Rodriguez, Matthias Perez, Kevin Billon, Jacky Mardjono, Vincent Clair, Manuel Collet

Accepted Manuscript
Version of Record available at: https://doi.org/10.1115/SMASIS2022-90914

NUMERICAL COMPUTATION OF THE ACOUSTIC RESPONSE OF AN ACTIVE AIRFOIL WITH IMPEDANCE BOUNDARY CONDITIONS TO A TURBULENT WAKE

Mouhamed Mounibe Ezzine[1,2,*], Jonathan Rodriguez[1], Matthias Perez[1], Kevin Billon[1], Jacky Mardjono[3], Vincent Clair[2], Manuel Collet[1]

[1]Université de Lyon, Ecole Centrale de Lyon, ENISE, ENTPE, CNRS, Laboratoire de Tribologie et Dynamique des Systèmes LTDS UMR5513, F-69134, Ecully, France
[2] Université de Lyon, Ecole Centrale de Lyon, INSA Lyon, Université Claude Bernard Lyon I, CNRS, Laboratoire de Mécanique des Fluides et d'Acoustique LMFA UMR5509, F-69134, Ecully, France
[3]Safran Aircraft Engines, F-75015, Paris, France

ABSTRACT

The noise generated by the interaction of the turbulent wake of the fan with the Outlet Guide Vanes (OGV) is a major component of turbofan engine noise. The development of noise reduction concepts applied to the OGV is an intensive research topic, with some current effort dedicated to an active solution making use of piezoelectric actuators integrated within the OGV airfoils to control the surface impedance. In order to define target values for the impedance that would lead to significant noise reduction over a chosen frequency range, a numerical method is being investigated in the present work. The method relies on solving the linearized Euler's equations in the frequency domain around an airfoil and introducing a velocity fluctuation representing the fan's turbulent wake upstream of the airfoil. An impedance boundary condition can be applied to the airfoil surface, and optimal values could be found through a parametric study. This paper presents the first set of 2D simulations that were performed to assess the capability of the method to show the effects of an impedance on the airfoil acoustic response, by comparison with a rigid one.

Keywords: Impedance, Aeroacoustics, Airfoil noise, piezoelectric shunt, Numerical simulation

NOMENCLATURE

Roman letters

c	Plate's chord length [m]
e	Plate thickness [m]
k_x	Wave number in the x direction [m^{-1}]
k_y	Wave number in the y direction [m^{-1}]
$\boldsymbol{n}$	outward unit normal vector [m]
p_0	Mean flow pressure [Pa]
p'	Pressure fluctuation [Pa]
R_s	Specific gas constant [$J.kg^{-1}.K^{-1}$]
SWL	Sound power level [dB]
T_0	Mean flow temperature [K]
$\boldsymbol{U_0}$	Mean flow velocity vector [$m.s^{-1}$]
$\boldsymbol{u'}$	Velocity fluctuation vector [$m.s^{-1}$]
Z_n	Normal impedance [$Pa.s.m^{-1}$]
S_c	Possible unsteady mass sources in the flow [$Kg.m^{-3}.s^{-1}$]
S_m	Possible unsteady acceleration sources in the flow [$m.s^{-2}$]
S_e	Possible unsteady pressure sources in the flow [$Pa.s^{-1}$]
I	Acoustic intensity [W]
c_0	Speed of sound in fluid [$m.s^{-1}$]
t	Time [s]

Greek letters

Δ	Mesh element size [m]
λ_{min}	Smallest wavelength [m]
ω	angular frequency [$rad.s^{-1}$]
ρ_0	Mean flow density [$kg.m^{-3}$]
ρ'	Density fluctuation [$kg\ m^{-3}$]

Dimensionless groups

ε	Relative amplitude of the gust [-]
γ	Specific heat ratio [-]
M	Mach number [-]

*Corresponding author: mounibe.ezzine@ec-lyon.fr

1. INTRODUCTION

The development of new solutions for reducing the radiated noise from the fan stage of turbofan engines has been an active research topic over the past decades [1, 2]. Most of the effort has been dedicated to passive technologies such as absorbing materials for intake liners [3, 4], but also low noise designs of the fan and stator blades [5–7].

These passive technologies, already available or under development, allow for significant reductions of fan noise at the operation points they have been designed for. Since the operating conditions of a turbofan engine are different at take-off, cruise or landing, passive technologies are usually not working optimally during at least one phase of the flight. Active and adaptive technologies may provide solutions able to reduce noise emissions for different operating conditions.

For this reason and in the context of the European project CleanSky2/InnoSTAT, an active airfoil with integrated piezoelectric transducers has been developed in order to reduce the noise emission due to the interaction of the turbulent wake of the fan with the Outlet Guide Vanes (OGV).

This study aims at investigating this active airfoil numerically, using an aeroacoustic model based on the linearized Euler equations, implemented in the finite element software COMSOL Multiphysics®, to compute the interaction with a turbulent wake. The effect of the piezoelectric transducers is represented here through an impedance boundary condition [8], applied to the surface of the airfoil. The first step of this work is to simulate the interaction between a monochromatic gust [9] and a thin rigid plate representing a simplified airfoil. Then, a set of simulations of gusts interacting with an airfoil making use of the impedance boundary condition is carried out. Several values of the impedance are considered to assess their effect on the emitted noise by the airfoil.

2. GEOMETRY AND MESH

The computational domain governed by linearized Euler equations is defined as a 2D square region of 8 m × 8 m represented in Figure 1. The domain is composed of two subdomains: (4) the central region where the interaction between the gust and the thin plate occurs, and (1) the PML(Perfectly Matched layer) surrounding the central region with a 1.5 m width on each side of the domain, used as a non-reflecting boundary condition for the wave equation.

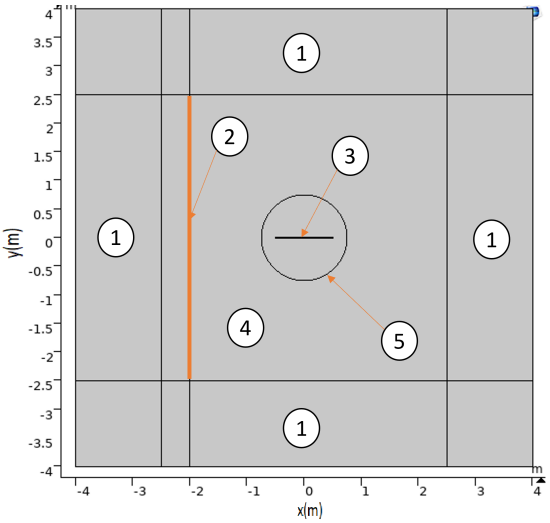

FIGURE 1: COMPUTATIONAL DOMAIN

The airfoil here is defined as a thin plate with a chord $c = 1$ m and a thickness $e = 0.02$ m. The leading and trailing edges of the plate are rounded. The center of the plate is located at the centre of the domain $(x, y) = (0, 0)$.

To ensure that the gust will be convected with little dissipation or dispersion through the physical domain, the mesh is defined with a maximum element size $\Delta = \lambda_{min}/25$, where λ_{min} is the smallest considered wavelength.

TABLE 1: NAME OF EACH COMPUTATIONAL DOMAIN REGION

Index	Region name
1	PML region
2	Injection boundary
3	Airfoil
4	Physical domain
5	Integration circle for sound power level

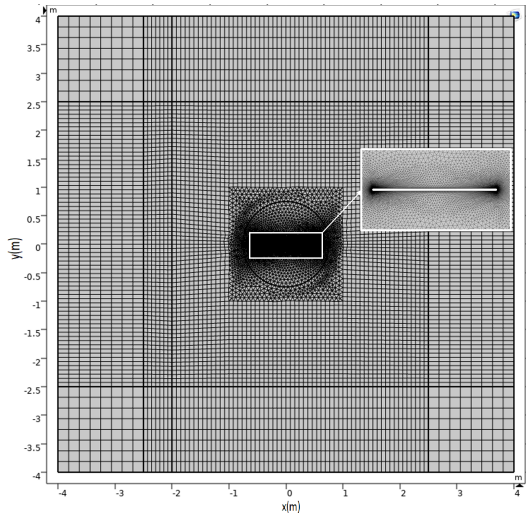

FIGURE 2: VIEW OF THE MESH, WITH ELEMENT SIZE INCREASED 132 TIMES FOR VISUALISATION.

3. LINEARIZED EULER'S EQUATIONS

The linearized Euler's equations are a set of equations that are commonly used to investigate the sound generation and propagation in aeroacoustics. The Euler's equations linearized around a stationary mean flow can be written as [10]:

Continuity equation:

$$\frac{\partial \rho'}{\partial t} + \nabla \cdot (\rho' \boldsymbol{U_0} + \rho_0 \boldsymbol{u'}) = S_c \tag{1}$$

Momentum equation:

$$\frac{\partial \boldsymbol{u'}}{\partial t} + \left(\left[\boldsymbol{u'} + \frac{\rho'}{\rho_0} \boldsymbol{U_0} \right] \cdot \nabla \right) \boldsymbol{U_0} + (\boldsymbol{U_0} \cdot \nabla) \boldsymbol{u'} + \frac{1}{\rho_0} \nabla p' = S_m \tag{2}$$

Energy equation, written for the pressure:

$$\frac{\partial p'}{\partial t} + \boldsymbol{u'} \cdot \nabla p_0 + p' \gamma (\nabla \cdot \boldsymbol{U_0}) + \boldsymbol{U_0} \cdot \nabla p' + \gamma p_0 (\nabla \cdot \boldsymbol{u'}) = S_e \tag{3}$$

The density ρ', the velocity $\boldsymbol{u'}$ and the pressure p' represent small perturbations around the mean flow of density ρ_0, velocity $\boldsymbol{U_0}$, and pressure p_0. γ refers to the specific heat ratio, and is taken as $\gamma = 1.4$ for air.

In the configuration considered here, the mean flow is uniform, with a velocity $\boldsymbol{U_0} = (U_0, 0)$, and there are no source terms, S_c, S_m or S_e. The problem considered is harmonic at an angular frequency ω, thus, equations (1) to (3) become:

$$-\mathrm{i}\omega \rho' + \nabla \cdot \rho_0 \boldsymbol{u'} = 0 \tag{4}$$

$$-\mathrm{i}\omega \boldsymbol{u'} + (\boldsymbol{U_0} \cdot \nabla) \boldsymbol{u'} + \frac{1}{\rho_0} \nabla p' = 0 \tag{5}$$

$$-\mathrm{i}\omega p' + \boldsymbol{u'} \cdot \nabla p_0 + \boldsymbol{U_0} \cdot \nabla p' + \gamma p_0 (\nabla \cdot \boldsymbol{u'}) = 0 \tag{6}$$

The origin of the noise generated in the present work is the interaction between the gust, which is a velocity fluctuation convected by the mean flow, and the airfoil (the plate). This problem has been widely studied in the literature for rigid airfoils, both analytically [11, 12] and numerically [9, 13]. The gust by itself must not be responsible for any noise generation, thus the gust's velocity fluctuation should satisfy a divergence free condition ($\nabla \cdot \boldsymbol{u'} = 0$). The gust is a monochromatic velocity fluctuation at an angular frequency ω, with a wave-vector $\boldsymbol{k} = (k_x, k_y)$. Since it the gust is simply convected by the mean flow $(U_0, 0)$, ω is related to the axial wavenumber by $\omega = k_x U_0$. The definition of the velocity fluctuation associated with the gust is [11]:

$$\begin{cases} u'_x = -\frac{\varepsilon U_0 k_y}{\sqrt{k_x^2 + k_y^2}} \mathrm{e}^{\mathrm{i}(k_x x + k_y y - \omega t)} \\ u'_y = \frac{\varepsilon U_0 k_x}{\sqrt{k_x^2 + k_y^2}} \mathrm{e}^{\mathrm{i}(k_x x + k_y y - \omega t)} \end{cases} \tag{7}$$

Where ε is the relative amplitude. The value of k_y has been set at $k_y = -k_x$ based on the definition of a benchmark gust-airfoil test case [9] and on previous work in the literature using the same value [13]. The gust as expressed in equation 7 is introduced in the computational domain along the line denoted (2) in figure 1.

4. RIGID AIRFOIL SIMULATIONS

In this section the interaction of a gust with a rigid thin plate is considered. The boundary condition corresponding to the rigid plate is a non-penetration condition defined on the surface of the plate as a zero normal velocity fluctuation:

$$\boldsymbol{u'} \cdot \boldsymbol{n} = 0 \tag{8}$$

All the parameters used in the study are described in the table 2.

TABLE 2: PARAMETERS USED

Parameter	Value	Unit
k_x	[40:1:120]	$[m^{-1}]$
c	1	$[m^1]$
$\boldsymbol{U_0}$	171.5	$[ms^{-1}]$
c_0	343	$[ms^{-1}]$
M	0.5	-
ε	0.02	-
p_0	1	[atm]
T_0	293.15	[K]
R_s	287.05	[J/kg K]
t	10	[s]

4.1 Results

The normal velocity fluctuation u'_y and the pressure fluctuation resulting from the interaction between the gust and the rigid plate are presented in figures 3 to 6 for two different gust wavenumbers. The radiated sound power is integrated over a circle surrounding the plate with a radius $R = 0.75$ m. It is defined as:

$$P = \int_\Omega \boldsymbol{I} \cdot \boldsymbol{n} \, \mathrm{dl} \tag{9}$$

With $\boldsymbol{I} = \frac{1}{2} Re(p' \boldsymbol{u'^*})$ the mean acoustic intensity vector, and $\boldsymbol{n}$ the outward unit vector normal to the integration surface.

The sound power level for the rigid case is presented in Figure 7 as a function of the axial wavenumber. The spectrum displays strong fluctuations and a large peak emerges for $k_x = -k_y = 56$ m^{-1} and for $k_x = -k_y = 79$ m^{-1}. In the following section, the value of the surface impedance on the airfoil will be investigated for axial wavenumbers around this value.

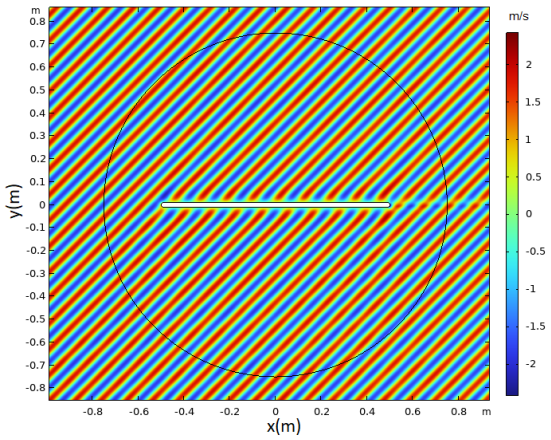

FIGURE 3: NORMAL VELOCITY FLUCTUATION u_y' FOR $k_x = -k_y = 56\ \mathrm{m}^{-1}$.

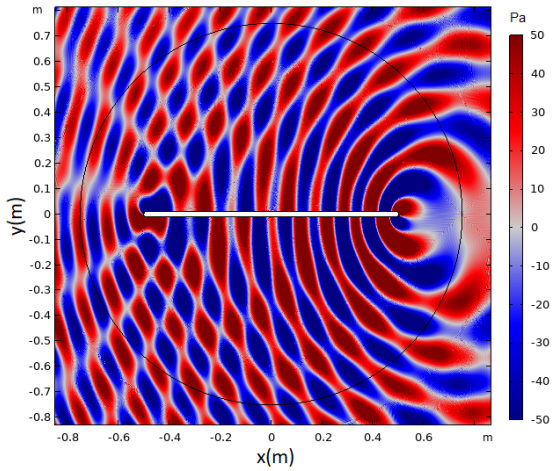

FIGURE 4: PRESSURE FLUCTUATION p' FOR $k_x = -k_y = 56\ \mathrm{m}^{-1}$.

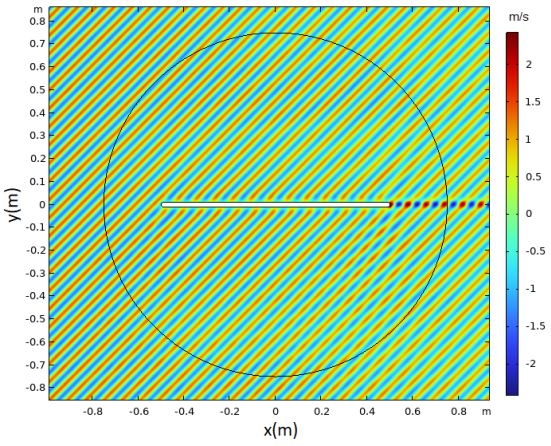

FIGURE 5: NORMAL VELOCITY FLUCTUATION u_y' FOR $k_x = -k_y = 79\ \mathrm{m}^{-1}$.

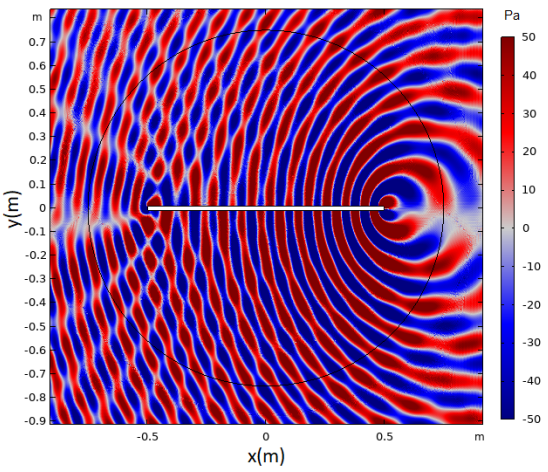

FIGURE 6: PRESSURE FLUCTUATION p' FOR $k_x = -k_y = 79\ \mathrm{m}^{-1}$.

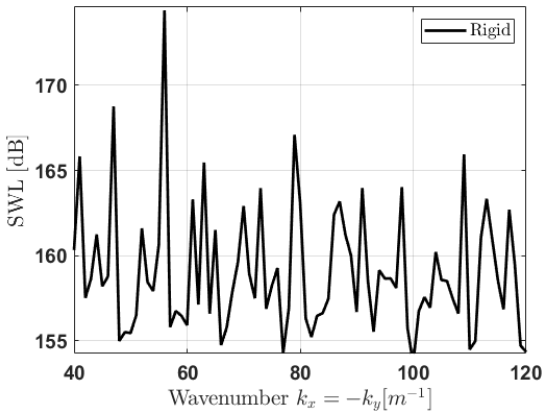

FIGURE 7: SOUND POWER LEVEL SWL [dB] EVOLUTION AGAINST WAVENUMBER $k_x = -k_y$ [m^{-1}].

5. EFFECT OF AN IMPEDANCE BOUNDARY CONDITION

After simulating the interaction of a gust with a rigid airfoil, an impedance boundary condition is now introduced at the surface of the airfoil. The objective of this section is to investigate the effects of different values of the impedance Z_n on the noise radiated. As mentioned above, in order to limit the number of simulations, the axial wavenumbers considered for the gusts will be restricted to values around $k_x = -k_y = 56\ \mathrm{m}^{-1}$ and $k_x = -k_y = 79\ \mathrm{m}^{-1}$. In the present work, only purely real values of the impedance will be considered ($Im(Z_n) = 0$), with values ranging from $Re(Z_n) = 1$ Pa.s.m^{-1} to 5 Pa.s.m^{-1}.

5.1 Impedance boundary condition

The non-penetration condition imposed on the surface of the airfoil for the rigid case as defined in equation (8) is replaced by a normal impedance boundary condition as expressed by Myers [8, 14] in the presence of a mean flow:

$$\boldsymbol{u'} \cdot \boldsymbol{n} = \frac{p'}{Z_n} + \frac{1}{i\omega}\boldsymbol{U_0}\nabla\left(\frac{p'}{Z_n}\right) - \frac{p'}{i\omega Z_n}\boldsymbol{n}\cdot(\boldsymbol{n}\cdot\nabla\boldsymbol{U_0}) \qquad (10)$$

For a uniform mean flow the mean flow gradient is equal to zero $\nabla\boldsymbol{U_0} = 0$ and the impedance boundary condition becomes:

$$\boldsymbol{u'} \cdot \boldsymbol{n} = \frac{p'}{Z_n} + \frac{1}{i\omega}\boldsymbol{U_0} \cdot \nabla \left(\frac{p'}{Z_n}\right) \tag{11}$$

5.2 Results

The results from the simulation performed for two gusts corresponding to both wavenumbers $k_x = -k_y = 56$ m^{-1} and $k_x = -k_y = 79$ m^{-1} with an impedance $Re(Z_n) = 3$ Pa.s.m^{-1} on the plate are shown respectively in figures 8 and 11for the normal velocity fluctuation and in figures 9 and 12 for the pressure fluctuation. When compared to the pressure fluctuation for a rigid plate shown in figure 4 for the two wavenumbers , the pressure levels radiated by the plate with an impedance have lower amplitudes. Some numerical artifacts that need some further investigation are visible on figures 9 and 12 for for both wavenumbers. The sound power level is calculated over the same surface as in the previous section, for several gust's axial wavenumbers and for several values of $Re(Z_n)$. The results are presented for the wavenumbers $k_x = -k_y = 56$ m^{-1} and $k_x = -k_y = 79$ m^{-1} respectively in figures 10 and 13. For all the values of $Re(Z_n)$, a reduction up to **12dB** of the sound power level can be observed for the wavenumber $k_x = -k_y = 56$ m^{-1}, in agreement with the pressure field shown in figure 9 for $Re(Z_n) = 3$ Pa.s.m^{-1}.While for the wavenumber $k_x = -k_y = 79$ m^{-1} we can observe a reduction up to **17dB** of the sound power level for the same value of impedance $Re(Z_n) = 3$ Pa.s.m^{-1}, in agreement with the pressure field shown in figure 12. The acoustic power is increased for a wavenumber $k_x = -k_y = 55$ m^{-1} and for all the considered impedances, especially for $Re(Z_n) = 1$ Pa.s.m^{-1}, which is the value with the weakest performances for this wavenumber. While for the wavenumber $k_x = -k_y = 79$ m^{-1} we observe that for $Re(Z_n) = 1$ Pa.s.m^{-1} we have the best result. Finally, the results for both wavenumbers show very little difference between the cases with impedances ranging from $Re(Z_n) = 2$ Pa.s.m^{-1} to 5 Pa.s.m^{-1}.

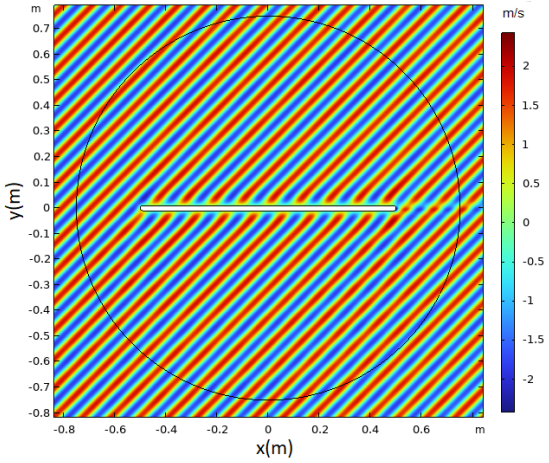

FIGURE 8: NORMAL VELOCITY FLUCTUATION u'_y FOR $k_x = -k_y = 56$ m^{-1} AND $Re(Z_n) = 3$ Pa.s.m^{-1}.

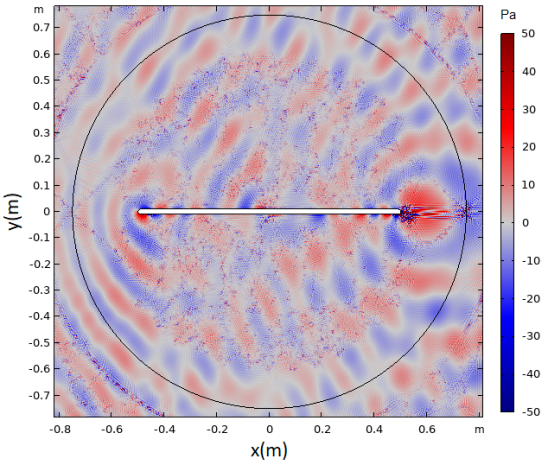

FIGURE 9: PRESSURE FLUCTUATION p' FOR $k_x = -k_y = 56$ m^{-1} AND $Re(Z_n) = 3$ Pa.s.m^{-1}.

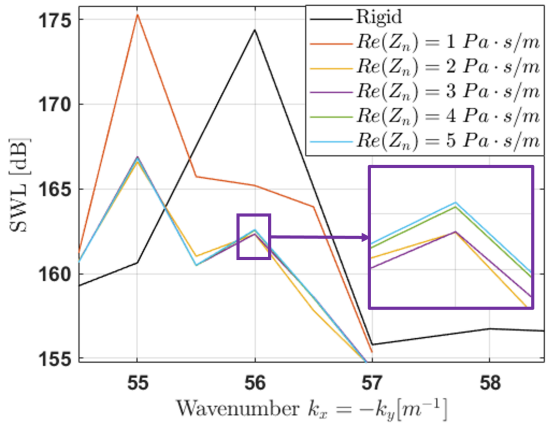

FIGURE 10: SOUND POWER LEVEL SWL [dB] EVOLUTION AGAINST WAVENUMBER $k_x = -k_y$ [m^{-1}] FOR DIFFERENT IMPEDANCE VALUE NEAR $k_x = -k_y = 56$ m^{-1}.

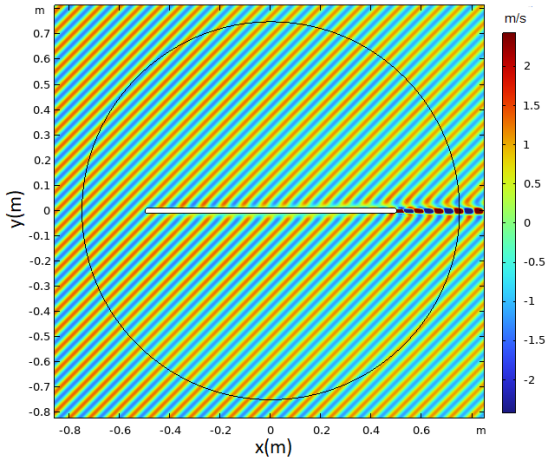

FIGURE 11: NORMAL VELOCITY FLUCTUATION u'_y FOR $k_x = -k_y = 79$ m^{-1} AND $Re(Z_n) = 3$ Pa.s.m^{-1}.

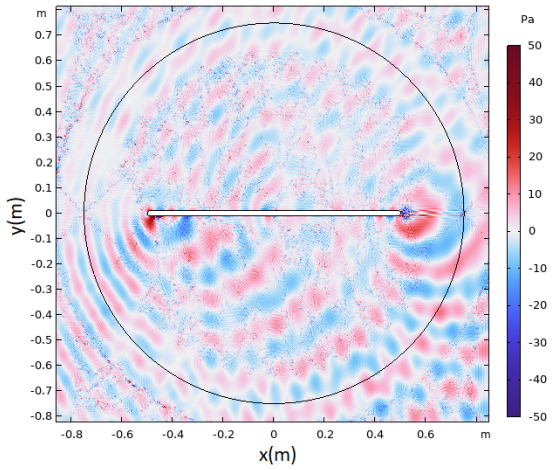

FIGURE 12: PRESSURE FLUCTUATION p' FOR $k_x = -k_y = 79$ m^{-1} AND $Re(Z_n) = 3$ Pa.s.m^{-1}.

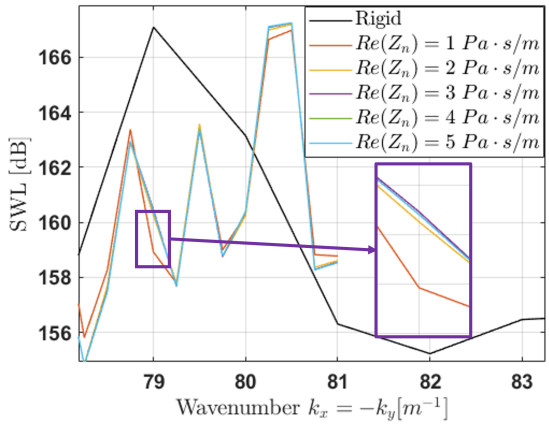

FIGURE 13: SOUND POWER LEVEL SWL [dB] EVOLUTION AGAINST WAVENUMBER $k_x = -k_y$ [m^{-1}] FOR DIFFERENT IMPEDANCE VALUE NEAR $k_x = -k_y = 79$ m^{-1}.

6. ACTIVE CONTROL PERSPECTIVES

The numerical method designed in this paper to include an impedance condition at the surface of an airfoil could be used in an optimization procedure. The optimal values of the impedance could then be found to minimize the noise radiated by the airfoil for a chosen set of axial wavenumbers (or frequencies). These optimal values could then become targets for an active airfoil noise reduction concept that is currently being developed. In this concept, piezoelectric transducers are integrated into active cells located close to the leading edge of an airfoil prototype, under an aluminum skin. The first electromechanical mode of these cells is used to maximize the system controllability within the desired frequency range. Since no pressure sensor is implemented into the system, only the impedance of the piezoelectric shunt is numerically controlled by measuring their voltage and controlling the current command signal in the circuit to target an equivalent acoustic impedance at the profile surface. This prototype is intended to be tested in a wind tunnel to confirm the control capacities to drive the multiple piezoelectric cells to the target acoustic impedance using numerical active piezoelectric shunt methods.

7. CONCLUSION

A computational aeroacoustics method, relying on the linearized Euler's equations solved in the frequency domain by a finite element solver, has been set up in 2D in the present work to study the noise generated by velocity fluctuations (gusts) impinging on an airfoil. This method allowed us to introduce a normal impedance onto the surface of the airfoil. A first set of simulations has been performed for a rigid airfoil (here a thin, flat plate) as well as for an airfoil with a purely real valued surface impedance. These simulations show that an effect of the impedance can be observed on the noise radiated. This effect can be strongly favorable for some velocity fluctuations' wavenumbers, but unfavorable for others. In future work, this methodology can be integrated in an optimization procedure to find impedance values that would result in significant noise reductions over a targeted range of wavenumbers (frequencies). This optimal impedance could then be reproduced by an active noise control concept using piezoelectric transducers integrated in an airfoil.

ACKNOWLEDGMENTS

This project has received funding from the Clean Sky 2 Joint Undertaking (JU) under agreement n°865007. The JU receives support from the European Union's Horizon 2020 research and innovation programme and the Clean Sky 2 JU members other than the Union. This publication reflects only the author's view and the JU is not responsible for any use that may be of the information it contains.

REFERENCES

[1] Envia, E. "Fan Noise Reduction: An Overview." *International Journal of Aeroacoustics* Vol. 1 No. 1 (2002): pp. 43–64.

[2] Moreau, S. "Turbomachinery Noise Predictions: Present and Future." *Acoustics* Vol. 1 No. 1 (2019): pp. 92–116.

[3] Marsh, A. "Study of Acoustical Treatments for Jet-Engine Nacelles." *The Journal of the Acoustical Society of America* Vol. 43 No. 5 (1968): pp. 1137–1156.

[4] Astley, R.J., Sugimoto, R. and Mustafi, P. "Computational aero-acoustics for fan duct propagation and radiation. Current status and application to turbofan liner optimisation." *Journal of Sound and Vibration* Vol. 330 No. 16 (2011): pp. 3832–3845.

[5] Chaitanya, P., Joseph, P., Narayanan, S., Vanderwel, C., Turner, J., Kim, J. W. and Ganapathisubramani, B. "Performance and mechanism of sinusoidal leading edge serrations for the reduction of turbulence–aerofoil interaction noise." *Journal of Fluid Mechanics* Vol. 818 (2017): p. 435–464.

[6] Polacsek, C., Cader, A., Buszyk, M., Barrier, R., Gea-Aguilera, F. and Posson, H. "Aeroacoustic design and broadband noise predictions of a fan stage with serrated outlet guide vanes." *Physics of Fluids* Vol. 32 No. 10 (2020): p. 107107.

[7] Bampanis, G. and Roger, M. "On the Turbulence-Impingement Noise of a NACA-12 Airfoil with Porous Inclusions." *Proceedings of the AIAA AVIATION 2020 FORUM*. 2020-2577.

[8] Myers, M. "On the acoustic boundary condition in the presence of flow." *Journal of Sound and Vibration* Vol. 71 (1980): pp. 429–434.

[9] Scott, J. "Third Computational Aeroacoustics (CAA) Workshop on Benchmark Problems: Category 3, Problem 1 – single airfoil gust response." NASA Technical Memorendum 2000-209790. NASA. 2000.

[10] Bailly, C. and Juvé, D. "Numerical solution of acoustic propagation problems using linearized Euler equations." *AIAA Journal* Vol. 38 No. 1 (2000): pp. 22–29.

[11] von Karman, T. and Sears, W. "Airfoil theory for non-uniform motion." *Journal of the Aeronautical Sciences* Vol. 5 No. 10 (1938): pp. 379–390.

[12] Amiet, R. "High frequency thin-airfoil theory for subsonic flow." *AIAA Journal* Vol. 14 No. 8 (1976): pp. 1076–1082.

[13] Scott, J. and Atassi, H. "A finite-difference, frequency-domain numerical scheme for the solution of the gust response problem." *Journal of Computational Physics* Vol. 119 (1995): pp. 75–93.

[14] Eversman, W. "The boundary condition at an impedance wall in a non-uniform duct with potential mean flow." *Journal of Sound and Vibration* Vol. 246 No. 1 (2001): pp. 63–69.

,